

# **Simulation of Forest Fire Spread with Different Methods**

**Team Number:** 11

Pranoy Ray  
Srikanth Avasarala  
Xiaodong An (Will)

**GitHub Repository:**

[https://github.gatech.edu/xan37/CSE-6730-Group-Project.](https://github.gatech.edu/xan37/CSE-6730-Group-Project)

**Video:**

[https://mediaspace.gatech.edu/media.](https://mediaspace.gatech.edu/media)

*Submitted for Final Report*

# Simulation of Forest Fire Spread with Different Methods

Group 11

December 3 2024

## 1 Abstract

Wildfires pose significant ecological and economic challenges, driven by complex interactions between vegetation, environmental factors, and atmospheric conditions. Understanding and predicting wildfire behavior is critical for effective mitigation and response strategies. In our project, we aim to explore the propagation dynamics using (i) Partial Differential Equations (PDEs), and (ii) Agent-based Cellular Automata model. This simulation provides a valuable tool for exploring the effects of environmental parameters and intervention strategies on wildfire behavior, contributing to better-informed decision-making in wildfire management.

## 2 Project description

The goal of our project is to simulate and analyze wildfire dynamics, along with strategies to mitigate their destructive impacts. We use two complementary approaches to model wildfire behavior: (i) solving Partial Differential Equations (PDEs) to capture continuous, large-scale fire spread dynamics and their interaction with environmental factors, and (ii) an Agent-based Cellular Automata model that simulates localized fire propagation based on individual tree states and environmental influences such as wind. Our agent-based model employs a grid-based representation of the forest, integrating multiple agents that affect the propagation dynamics and adjusting fire spread dynamically. We finally apply our model to investigate the wildfire propagation on a real-dataset based on 2018 California fires. Therefore our modeling approaches enable us to investigate the interplay between environmental parameters, intervention strategies, and fire behavior. By simulating propagation scenarios, we could ultimately decide on actionable insights for wildfire prevention and management, ultimately reducing ecological damage and safeguarding human communities.

## 3 Literature survey

### 3.1 Problem definition

Forest fires are one of the most destructive natural disasters, characterized by their sudden onset, extensive damage, and increasing frequency due to climate anomalies and uneven precipitation patterns. For example, China experienced 709 forest fires in 2022, affecting 5,000 hectares, with Yunnan Province being particularly vulnerable due to its vegetation, high temperatures, and mountainous terrain. These fires not only destroy habitats and render soil infertile but also contribute significantly to air pollution, with 30 percent of atmospheric CO<sub>2</sub> attributed to wildfires. The 2019-2020 Australian mega-fire, which burned 97,000 km<sup>2</sup>, exemplifies the devastating ecological and economic impact of wildfires. Forests, essential for oxygen production, biodiversity, and global economies, face critical threats from these events. Effective forest fire management requires understanding the complex physical and chemical processes governing fire spread, influenced by flammability, weather, and terrain. Advanced computer simulations and early detection technologies, such as thermal cameras, satellite systems, and UAVs, are crucial tools for predicting fire spread and supporting timely interventions to mitigate catastrophic consequences.

### 3.2 Existing models and techniques

Forest fire spread models can be broadly categorized into physical, empirical, and semiempirical approaches based on the equations governing them. Physical models emphasize detailed mechanisms such as heat transfer, combustion, and fluid dynamics. Examples like the Weber model in Australia are highly accurate but computationally demanding, as they require solving complex systems of equations [1]. Empirical models, on the other hand, derive simplified equations from observed fire behaviors, focusing on parameters like fire spread rates. Examples include the McArthur model in Australia [2] and the Wang Zhengfei and Mao Xianmin models in China [3, 4]. Semiempirical models strike a balance by combining theoretical underpinnings with experimental calibration to estimate parameters. A key example is the Rothermel model in the U.S., widely used for operational fire management [5].

Advancements in computational capabilities have shifted attention toward simulation models, which fall into discrete (e.g., cellular automata, CA) and continuous (e.g., PDE-based) categories [6]. CA models represent landscapes as grids, with transition rules dictating fire spread based on neighbor interactions. The classical Drossel-Schwabl model [7] introduced Monte Carlo simulations to study spatiotemporal fire dynamics. Extensions of CA models, such as Chopard et al.'s random walk simulation [8] and Karafyllidis and Thanailakis' wind- and terrain-sensitive model [9], improved their applicability to real-world scenarios. Stochastic CA models further advanced the field, incorporating probabilistic ignition and geometric rules for more realistic fire fronts [10, 11].

PDE-based models, in contrast, provide a continuous framework for simulating variables like temperature, fuel consumption, and heat flux. Early work by Montenegro et al. [12] demonstrated how factors like fuel type, moisture, and wind could be integrated using finite difference and finite element methods. Simplified models, such as those by Asensio et al. [13], focused on dominant heat transfer mechanisms and conservation laws, while Ferragut et al. [14] coupled meteorological data for improved accuracy. Advanced numerical techniques, such as adaptive grid refinement, Kalman filters, and Crank-Nicholson methods, have further enhanced the predictive power of PDE models [15, 16].

### 3.3 Our contribution

While CA models excel in computational efficiency and capturing complex spatial patterns, PDE models offer detailed insights into fire dynamics and physical processes. This study leverages the strengths of both approaches. We employ a multi-agent CA model incorporating transition rules for discrete CA states by accounting for environmental heterogeneity, such as vegetation and wind patterns. Simultaneously, we formulate a PDE-based framework that integrates topographical effects, wind dynamics, and combustion kinetics. To assess the reliability and applicability of these models, we validate and test them while using real-world data from the 2018 California wildfires, ensuring their effectiveness in simulating real fire scenarios and providing actionable insights.

## 4 Conceptual model

We use two conceptual models (i) PDE -based model (ii) Agent-based CA model. The model description for both are stated in the below section.

### 4.1 PDE-based model

While Cellular Automata focuses on the transition law between neighboring cells within certain landscape [17], PDE emphasizes more on the side of physical law. By generalizing the forest fire phenomenon with certain PDEs based on dynamical principles, we can solve the forest fire problem with a deeper understanding of its dynamics. By far, many PDE models have been suggested, as shown in [12, 13, 14, 15, 18], with most of them having finite difference and Euler methods applied to solve spatial correlation and to integrate over time. However, as noted by Martin & Torres [17], it is challenging to reproduce the codes of

methods mentioned above. Therefore, we adopt a relatively more simplified and accessible one as outlined in [17].

In a 2D map  $\Omega$ , we have the pixel  $\mathbf{x}$  to be:

$$\mathbf{x} = (x, y) \in \Omega = [x_{\min}, x_{\max}] \times [y_{\min}, y_{\max}],$$

with the boundary  $\partial\Omega$  defined as:

$$\partial\Omega \equiv \Gamma.$$

Now the PDEs describing the state of forest fire are:

$$\begin{aligned}\mathbf{v}(\mathbf{x}, t) &= \mathbf{w}(t) + \nabla Z(\mathbf{x}), \\ \dot{u}_t &= \kappa \Delta u_t - \mathbf{v} \cdot \nabla u_t + \mathcal{H}(u_t - u_{pc}) \beta \exp\left(\frac{u_t}{1 + \varepsilon u_t}\right) - \alpha u_t, \\ \dot{\beta}_t &= -\mathcal{H}(u_t - u_{pc}) \frac{\varepsilon}{q} \beta \exp\left(\frac{u_t}{1 + \varepsilon u_t}\right),\end{aligned}$$

Where  $\dot{u}_t = \dot{u}(t)$  is the temperature change rate,  $\dot{\beta}_t = \dot{\beta}(t)$  is the fuel change rate,  $\mathbf{v} = \mathbf{v}(\mathbf{x}, t)$  is the velocity field at a given point in space and time,  $\mathbf{w}(t)$  represents the effect of wind,  $Z(\mathbf{x})$  is the topography,  $\kappa$  is the diffusion coefficient,  $\varepsilon$  is the inverse of the activation energy,  $q$  is the reaction heat,  $\alpha$  is the natural convection coefficient,  $u_{pc}$  is the phase change threshold,  $\nabla$  is the gradient operator,  $\Delta$  is the Laplacian operator, and  $\mathcal{H}()$  is the Heaviside step function. In reference [19], it shows the typical activation energy used here is  $E_A \approx 20$  kcal/mol or  $\epsilon$ (with unit)  $\approx 0.05$  mol/kcal. The simulation time describes approximately 200 time steps per day.

The initial conditions include:

$$\begin{aligned}\mathbf{w}(t), Z(\mathbf{x}), \\ \mathbf{u}(\mathbf{x}, 0) &= u_0(\mathbf{x}), \\ \boldsymbol{\beta}(\mathbf{x}, 0) &= \beta_0(\mathbf{x}).\end{aligned}$$

In another words

With a pre-setting that forest fire will not spread outside  $\Omega$ , we have the Dirichlet boundary conditions as follows:

$$u_\Gamma(\mathbf{x}, t) = \beta_\Gamma(\mathbf{x}, t) = 0$$

A summary of the state variables and map can be seen in Fig. 1

The model described above provides a mathematical framework for simulating the dynamics of forest fires, taking into account both physical laws and environmental factors such as wind, topography, and fuel conditions. By solving the coupled PDEs for temperature and fuel change, we can gain insights into the behavior and spread of the fire across the landscape. The initial and boundary conditions further define the problem setup, ensuring that the simulation remains realistic and applicable to real-world scenarios.

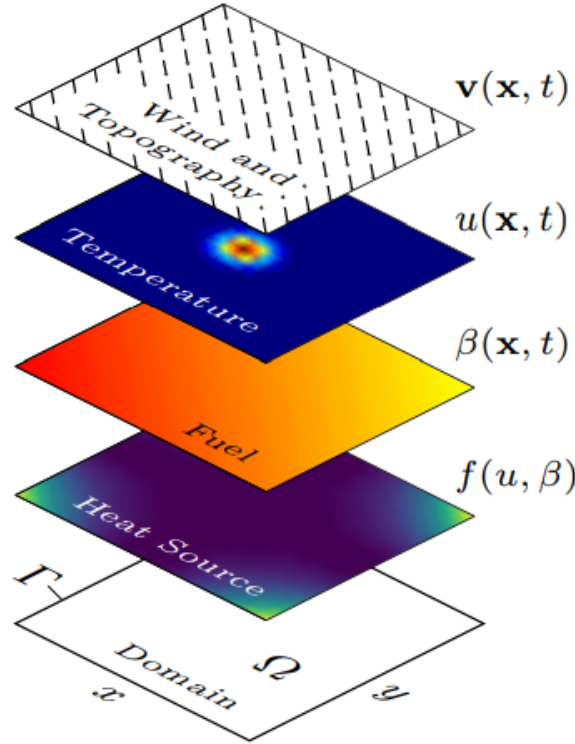


Figure 1: Visualization of the state variables and spatial map in the forest fire simulation using the PDE method [17].

#### 4.1.1 Numerical Implementation of the PDE-based Model

The simulation is coded in Python and its physical domain is numerically calculated using meshgrid from numpy library with uniform spacing  $\Delta x$  and  $\Delta y$ . Time evolution is computed with a time step  $\Delta t$ , and its value is chosen to satisfy the Courant–Friedrichs–Lewy (CFL) condition to ensure numerical stability [17]. The state variable  $u(i, j, n)$  and  $\beta(i, j, n)$  is discretized as  $u_{i,j}^n$  and  $\beta_{i,j}^n$ , where  $i$  and  $j$  are the spatial locations, and  $n$  is the current simulation time step.

The governing PDE is discretized using a central difference scheme for spatial derivatives and a forward Euler scheme for time integration.

For the time integration, suppose a generic PDE::

$$\frac{\partial u_{i,j}^n}{\partial t} = f(u^n),$$

the forward eular can be expressed as:

$$\frac{u_{i,j}^{n+1} - u_{i,j}^n}{\Delta t} = f(u^n).$$

Then, the time evolution is:

$$u_{i,j}^{n+1} = u_{i,j}^n + \Delta t \cdot f(u^n).$$

For the gradient and laplacian operators:

$$\nabla_x u_{i,j}^n = \frac{u_{i+1,j}^n - u_{i-1,j}^n}{2\Delta x}, \quad \nabla_y u_{i,j}^n = \frac{u_{i,j+1}^n - u_{i,j-1}^n}{2\Delta y}.$$

$$\nabla^2 u|_{i,j} = \frac{u_{i+1,j} - 2u_{i,j} + u_{i-1,j}}{\Delta x^2} + \frac{u_{i,j+1} - 2u_{i,j} + u_{i,j-1}}{\Delta y^2}.$$

The boundary condition uses the Dirichlet condition.

## 4.2 Agent-based CA model

The Agent-based CA model is inspired off of works [20, 21]. This model simulates forest fire spread using cellular automata (CA), a framework based on a grid of cells that evolve in discrete time steps. Each cell represents a patch of forest, and its state changes depending on local environmental factors and interactions with neighboring cells. The model incorporates influences from combustibles, meteorological conditions, terrain, and time to capture the complex dynamics of fire propagation which act as *agents* for the model.

The grid consists of each cell with a state representing its fire condition: unburned, ignited, burning, extinguishing, or extinguished. State transitions are governed by predefined rules and depend on the cell's neighbors within a Moore neighborhood (the eight surrounding cells).

The spread rate of forest fires is influenced by various factors, including the type and moisture content of combustible materials, meteorological conditions, and the topography and terrain of the affected area. Typically, this rate is determined through experimental measurements.

The formula for calculating the forest fire spread rate is expressed as:

$$R = R_0 K_S K_W K_\theta$$

where  $R$  is the spread rate ( $m/min$ ),  $R_0$  is the initial spread rate ( $m/min$ ),  $K_S$  is the combustible material configuration coefficient,  $K_W$  is the wind correction coefficient, and  $K_\theta$  is the terrain correction coefficient.

The initial spread rate,  $R_0$ , is influenced by temperature, wind speed, and relative humidity. Wang Zhengfei derived a relationship based on field ignition experiments, expressing  $R_0$  as a function of these variables. The formula is given as:

$$R_0 = aT + bV + c(1 - RH) - D$$

where  $R_0$  is the initial spread rate ( $m/min$ ),  $T$  is the daily maximum temperature ( $^\circ C$ ),  $V$  is the average wind speed at noon ( $m/min$ ), and  $RH$  is the relative humidity (%). The coefficients are defined as:

$$a = 0.03, \quad b = 0.05, \quad c = 0.01, \quad D = 0.3.$$

The wind coefficient,  $K_W$ , incorporates the influence of wind speed and direction on the rate of forest fire spread. It is expressed as:

$$K_W = e^{0.1783v \cos \phi}$$

where  $v$  is the wind speed ( $m/s$ ) and  $\phi$  is the angle between the wind direction and the direction of fire spread ( $^\circ$ ). This coefficient increases the spread rate when the wind aligns with the fire spread direction ( $\phi = 0^\circ$ ) and decreases it when the wind opposes the fire's progression ( $\phi = 180^\circ$ ). Next, the terrain correction coefficient  $K_\theta$  is computed as

$$K_\theta = e^{3.553gtan^{1.2}\theta}$$

$g$  is the direction of the hill (1 for uphill and -1 for downhill). The slope angle,  $\theta$ , which determines the impact of terrain on fire spread, is calculated using the formula:

$$\theta = \arctan \left( \frac{A_{ij} - A}{\sqrt{(x_i - x)^2 + (y_j - y)^2}} \right)$$

where  $A_{ij}$  is the elevation of the neighboring cell (m),  $A$  is the elevation at the fire ignition point (m),  $(x, y)$  are the coordinates of the fire ignition point, and  $(x_i, y_j)$  are the coordinates of the neighboring cell.

Uphill terrain, where  $\theta > 0$ , promotes faster fire spread as flames and heat are directed toward unburned fuel upslope, enhancing combustion. Conversely, downhill terrain, where  $\theta < 0$ , inhibits fire spread since heat and flames move away from the unburned fuel, reducing the rate of spread.

#### 4.2.1 Geographic Cellular Automata Algorithm

Cellular automata are dynamic systems defined in cellular space, characterized by discrete finite-state compositions that evolve according to local rules over discrete time steps (Collin et al., 2011). Formally, these are defined by an  $n$ -dimensional cellular space, the state, the number of neighborhoods, and state transition rules  $(\mathbb{Z}^n, S, N, f)$ .

In the forest fire spread geographic cellular automata (CA) algorithm, the geographic cell space ( $\mathbb{Z}^n$ ) consists of fire units with varying geographic combustion conditions ( $S$ ). The evolution of the system is governed by state transition rules  $S_{t+\Delta t} = f(S_t, N)$ , which define the state of each cell based on its current state and the states of its Moore neighborhood ( $N$ ).

Therefore, the CA algorithm represents the cells as a grid of pixels where each pixel value corresponds to a cell state. Assuming  $S$  is the state of a cell, it can take the following values:  $S = 0$  (unburned),  $S = 1$  (early burning),  $S = 2$  (fully burning, capable of igniting neighboring cells),  $S = 3$  (extinguishing), and  $S = 4$  (extinguished).

After initializing the fire information and time, cells in state  $S = 2$  ignite combustible neighboring cells, simulating forest fire spread. The evolution of time is discrete, and the fire state at  $t + \Delta t$  is determined based on the state at time  $t$ . The state evolution is expressed as follows:

---

**Algorithm 1** State Evolution in Forest Fire Spread Cellular Automata Algorithm

---

**Require:** Initial cell states  $S_t$  for all cells in the grid, Moore neighborhood  $N$

**Ensure:** Updated cell states  $S_{t+\Delta t}$  for all cells until the fire is extinguished

```

0: while there exists any cell  $S < 4$  do {Continue until all cells are extinguished}
0:   for each cell  $(i, j)$  in the grid do
0:     if  $S_t^{i,j} = 0$  and any neighbor cell  $(i', j')$  has  $S_t^{i',j'} = 1$  then
0:        $S_{t+\Delta t}^{i,j}$  updated using eq. 1 {Ignite unburned cell}
0:     else if  $S_t^{i,j} = 1$  then
0:        $S_{t+\Delta t}^{i,j} \leftarrow 2$  {Transition to fully burning}
0:     else if  $S_t^{i,j} = 2$  and all neighbors are  $S \geq 2$  or non-combustible then
0:        $S_{t+\Delta t}^{i,j} \leftarrow 3$  {Start extinguishing}
0:     else if  $S_t^{i,j} = 3$  then
0:        $S_{t+\Delta t}^{i,j} \leftarrow 4$  {Completely extinguished}
0:     end if
0:   end for
0:   Update all cell states  $S_t \leftarrow S_{t+\Delta t}$ 
0: end while=0

```

---

The process of state transition is governed by the following equations:

$$S_{t+\Delta t}^{i,j} = S_t^{i,j} + \frac{\sum R_t^{i',j'} \Delta t}{L}, \quad R_t^{i,j} = 0, \quad (1)$$

where  $(i', j')$  are Moore neighbors of  $(i, j)$ .

$$\Delta t = m \frac{L}{R_{\max}}, \quad (m < 1), \quad (2)$$

where  $\Delta t$  is the time step,  $t$  is the current time,  $t + \Delta t$  is the next time step,  $(i, j)$  represents the cell location,  $S_{t+\Delta t}^{i,j}$  is the state of cell  $(i, j)$ .  $L = 30m$  is the cell size in the grid.  $R_{\max}$  is the maximum chosen rate of fire propagation in  $m/min$ . If  $S_{t+\Delta t}^{i,j} \geq 1$  from the above equation, then the value of  $S_{t+\Delta t}^{i,j}$  is set to be equal to 1.

## 5 Simulation Setup

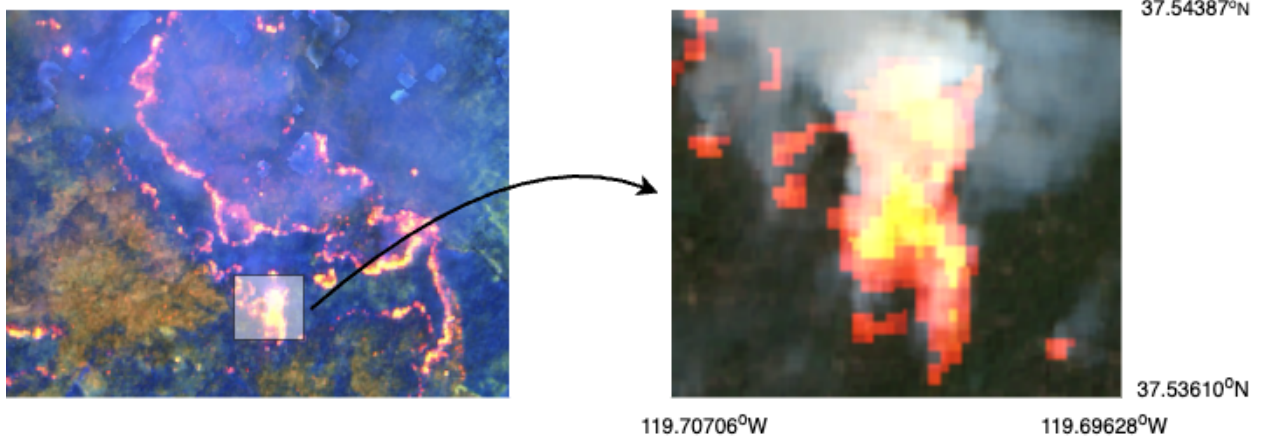


Figure 2: Satellite Lidar-1A image of Geographical region of interest chosen for the study - i.e latitudes  $37.53610^{\circ}\text{N}$  to  $37.543871^{\circ}\text{N}$  and longitudes  $119.69628^{\circ}\text{W}$  to  $119.70706^{\circ}\text{W}$  representing a region from the Mariposa County in California, taken on 5th August 2018.

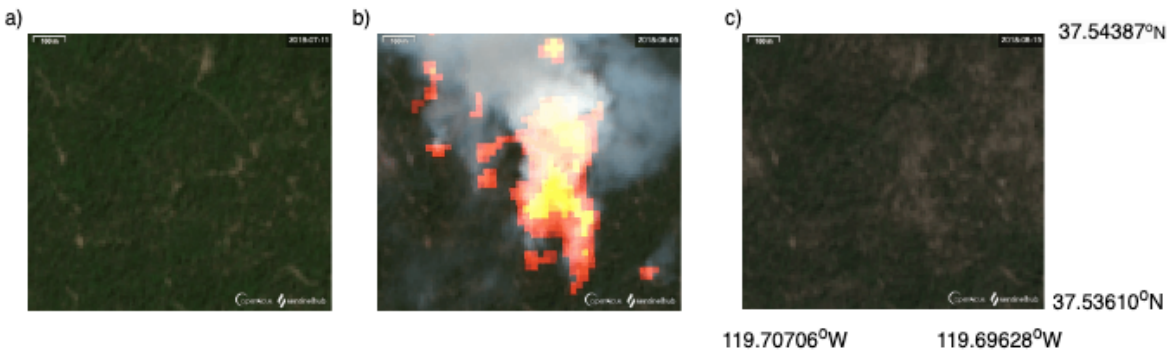


Figure 3: Satellite Lidar-1A image of Geographical region of interest chosen for the study under different stages - a) unburned - 11th July 2018, b) burning - 5th August 2018, and c) burned - 15th August 2018.

### 5.1 Data Acquisition

The dataset for this study is derived from the Ferguson Fire, a significant 2018 wildfire in Mariposa County, California, reportedly ignited by superheated fragments from a vehicle's catalytic converter. We utilize Sentinel Hub [22] for satellite images, specifically Sentinel Level-1A (L1A) data of 20m resolution, which retains raw radiometric and geometric properties. The study region spans latitudes  $37.543871$  to  $37.53610$  and longitudes  $-119.70706$  to  $-119.69628$  (Fig. 2), with images extracted from July 11 to August 15, 2018. Satellite data is sparse across time due to factors like cloud cover, smoke, and orbit patterns. As a result, we could only get satellite images at three relevant stages of the wildfire. The closest image to the event of burning was taken on July 11 2018, which we later use as an initial condition for state for both PDE and

ABM models. The second image we have is during active burning shown in fig. 3b, taken on 5th August 2018, and the last image fig. 3c is time closest to the end of wildfire in the geographical area under study.

Meteorological data—including wind speed and direction, maximum relative humidity, and temperature—are integrated into the model. The terrain data, sourced from a DEM[23], is processed into a NumPy array with an elevation range of 91–3959 m. Sparse satellite images prevent pinpointing the exact ignition points; likely locations are inferred from firefront development. Based on meteorological data from the study region [24], we use a average wind speed of 2.2 m/s at 260° angle, a temperature of 27°C, and relative humidity of 40%, recorded during peak afternoon conditions. We note that the above meteorological conditions fluctuate throughout the simulation time, but are assumed constant in order to accommodate the above variables seamlessly into the simulation model. We later also plot simulation sensitivities to some of these variables.

## 5.2 Initial Firing Position

To identify the initial firing positions, we analyzed the image as shown in Fig. 4, where the red dots mark the detected firing locations. We also applied an RGBa filter, which was defined with a lower boundary of [230, 0, 0, 0] and an upper boundary = [300, 80, 80, 300]. So that we can get the indices of initial firing locations in the image array. The implementation of the initial fire used Gaussian distribution, where for example, at firing locations  $[(x_0, y_0), (x_1, y_1)]$ , we have  $u^0(x, y) = 6e^{-0.05((x-x_0)^2+(y-y_0)^2)} + 6e^{-0.05((x-x_1)^2+(y-y_1)^2)}$

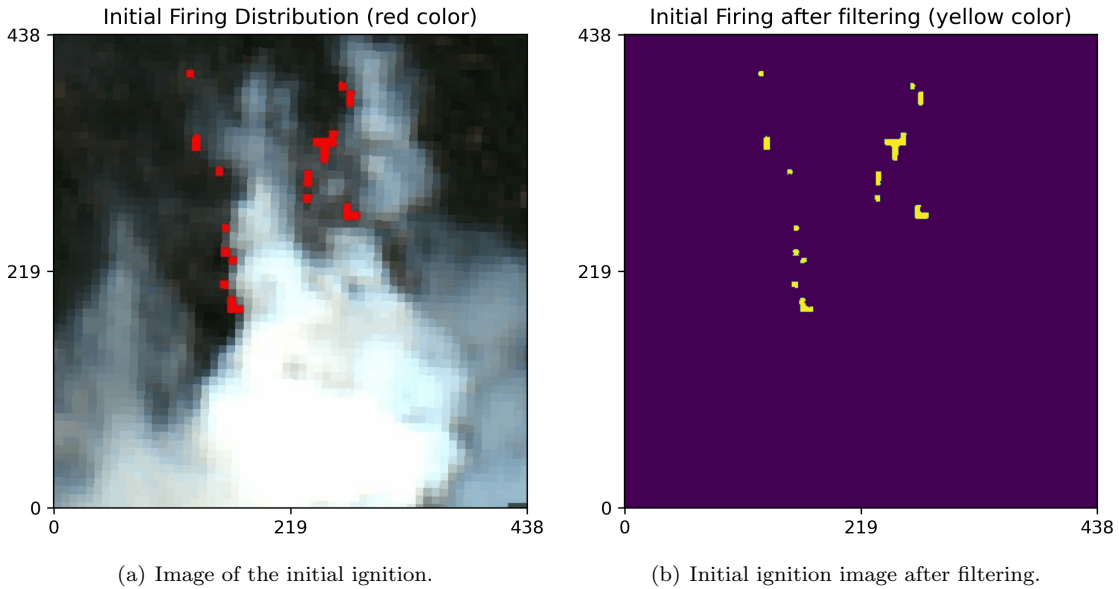


Figure 4: Satellite image of the probable region where the ignition began, based on the maximum burn ratio measured in the satellite image taken on August 5th 2018- a) represents the original image, and b) is the filtered image.

## 5.3 Wind and Topography Condition

From the data, the wind speed during this period was 2.2 m/s, while the topography is visualized in Fig.5(a). Both the wind and topography data were normalized, and their combined effects are represented as directional arrows in Fig.5(b).

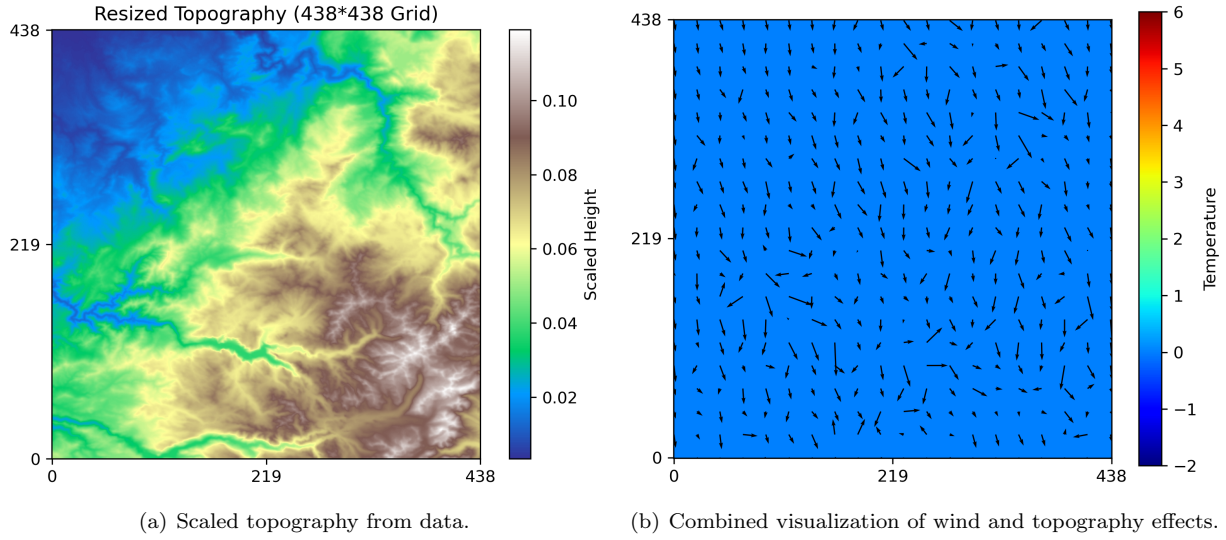


Figure 5: Initial wind and topology scaled.

#### 5.4 Initial Fuel Distribution

Frame 1 (Fig 9(a)) from the data source (GIF) shows the forest before the fire happened. To analyze the image, we extract the RGB values of each pixel. A threshold of  $\text{RGB} = \{52, 0, 0\}$  is defined to identify fuel regions: any pixel with RGB values exceeding this threshold is seen as a non-fuel pixel. For pixels identified as fuel, the fuel intensity is scaled to their G-channel (green) values. The scaled fuel intensity is depicted in Fig 9(b).

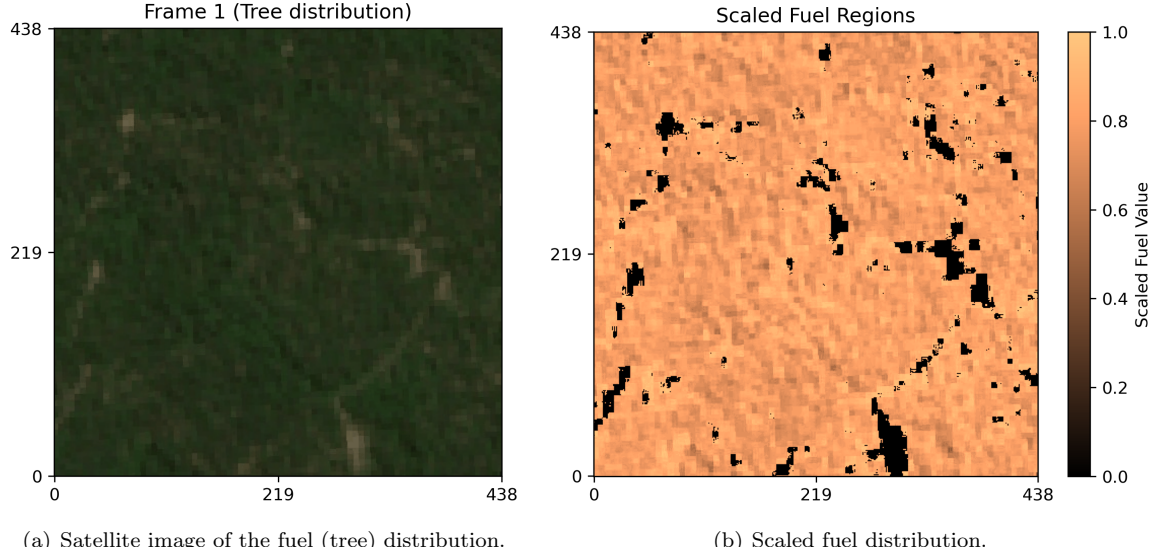


Figure 6: Initial fuel distribution - both satellite image and processed image, leading to a scaled fuel distribution.

## 6 Experimental Results

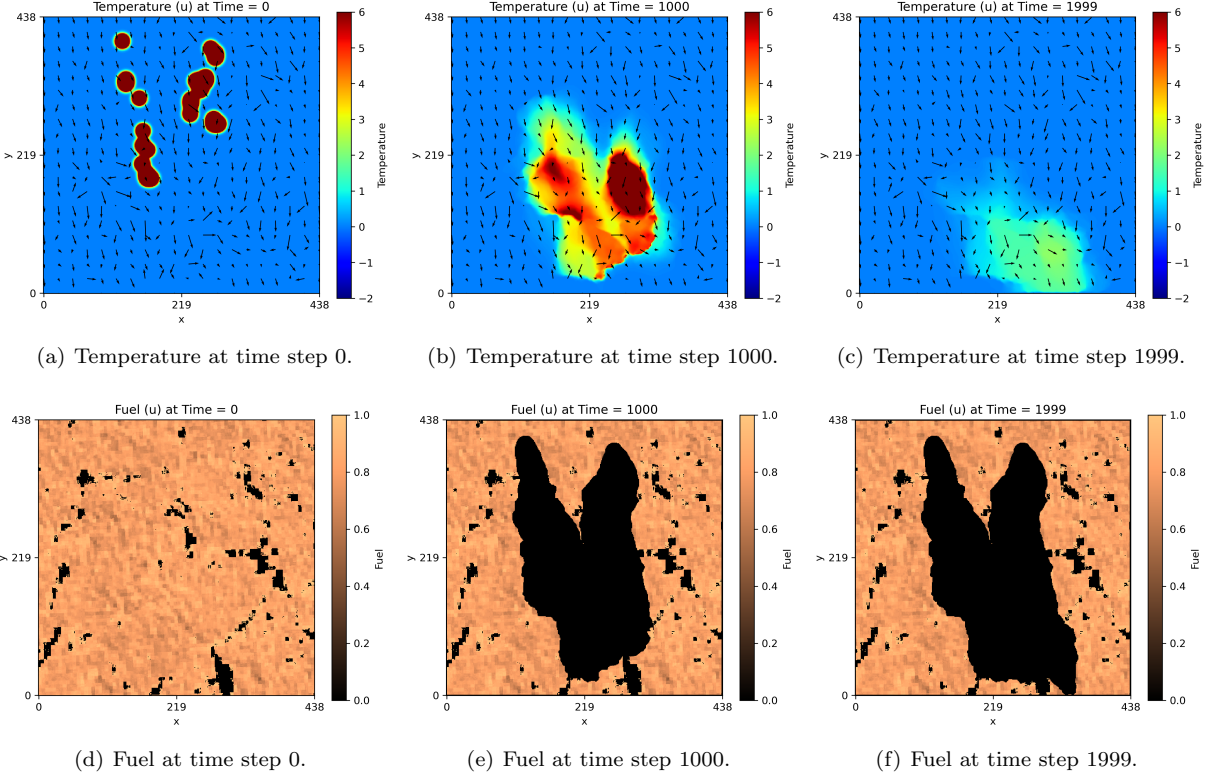


Figure 7: Results for PDE model.

### 6.1 PDE

Fig 7 presents the results obtained from the PDE model. At time step 0, the initial fire is depicted as a Gaussian distribution, highlighted in red. By time step 1000, by the effect of wind and topography, the fire goes to the south, consistent with the pattern illustrated in Fig 2, where the fire progresses similarly to the south.

The fire largely ends at around time step 2000, as shown in Fig 8(c), where most of the temperature dissipates to zero. Furthermore, the total fuel consumption depicted in Fig 7(f) demonstrates the complete fire track, with the left-side fire burning slightly faster.

Due to the space limit, we did not include additional simulation steps in this report. For more details, please access the Jupyter Notebook available in the Git repository, where you can run the simulation to explore further.

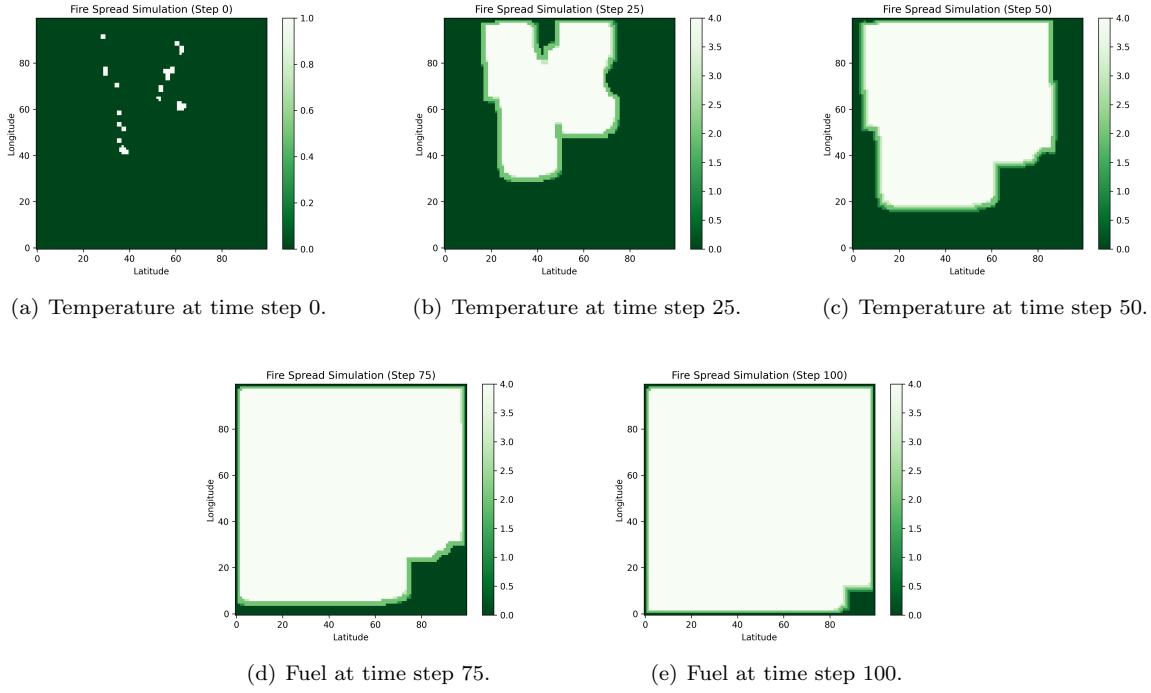


Figure 8: Results for ABM model. Green spots indicate unburnt areas.

## 6.2 ABM

Fig. 8 shows the time evolution plot of the CA states across time for the default chosen parameters of wind, terrain, and meteorological conditions followed by hyperparameters specific to the ABM setup. As expected, we see the that with time, the firefront propagates converting the unburned area to burned area. We observe that the firefront is more radial or spherical than the one observed with PDE which has a butterfly like shape stemming from tthe assymetry casued by terrain and wind conditions which are captured more efficiently by the PDE model as compared to the ABM model that we use, since the PDE model captures the physics of the phenomenon, where as the employed ABM model on the other hand is more meta-heuristic and simplified. We next plot the sensitivity plots for the burned are with time with respect to some of the important agents, like combustibility - which is a function of the vegetation type, since we do not have consistent information about the kind of vegetation and the combustibility factor  $K_S$  data (this corresponds to the inverse activation energy in PDE) , we assume it to be equal to 1. In the next section, we also perform sensitivity analysis for a range of combustibility values.

### 6.3 Validation

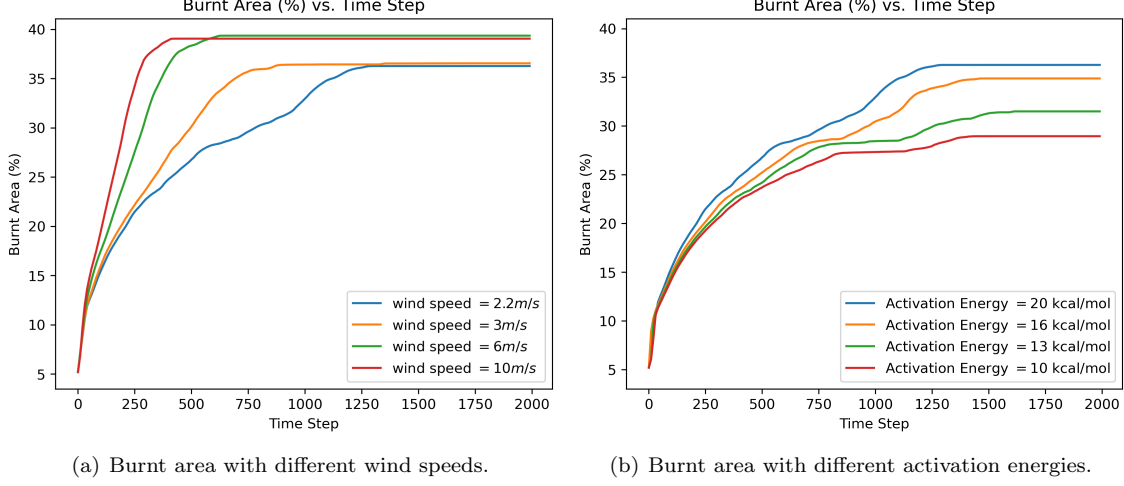
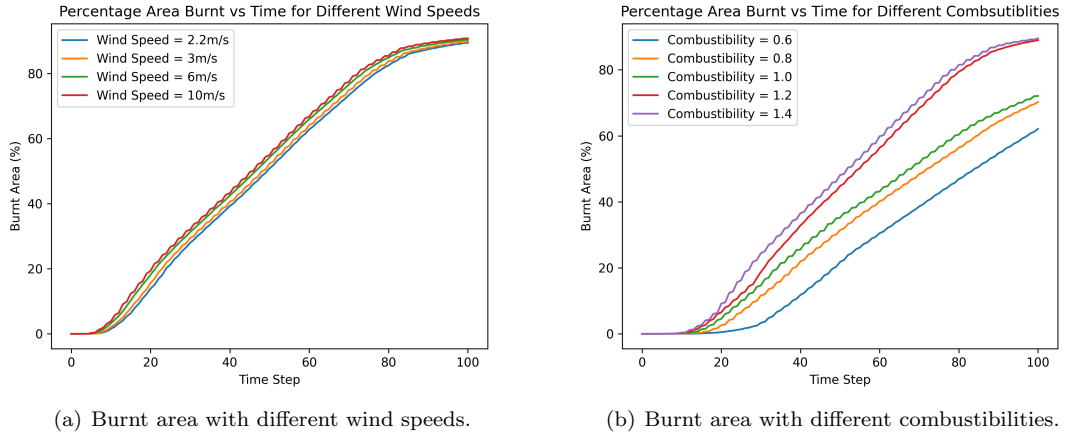


Figure 9: PDE Analysis.

In Figure 11(b), we scaled the after-burnt tree distribution and got the percentage of burnt area  $\approx 36.68\%$ , closely matching the PDE model result in Figure 7(f) ( $\approx 36\%$ , which is also the blue curve in Figure 9(a)). However, the ABM result in Figure 10(b) ( $\approx 80\%$ ) does not have a good match. While the models show good performance in estimating the overall burnt area, there is a noticeable difference in the exact shape of the burnt region. The difference is mainly due to the simplicity of our models and the limitations of data sources, including low-resolution satellite images and unreliable internet sources for weather conditions.

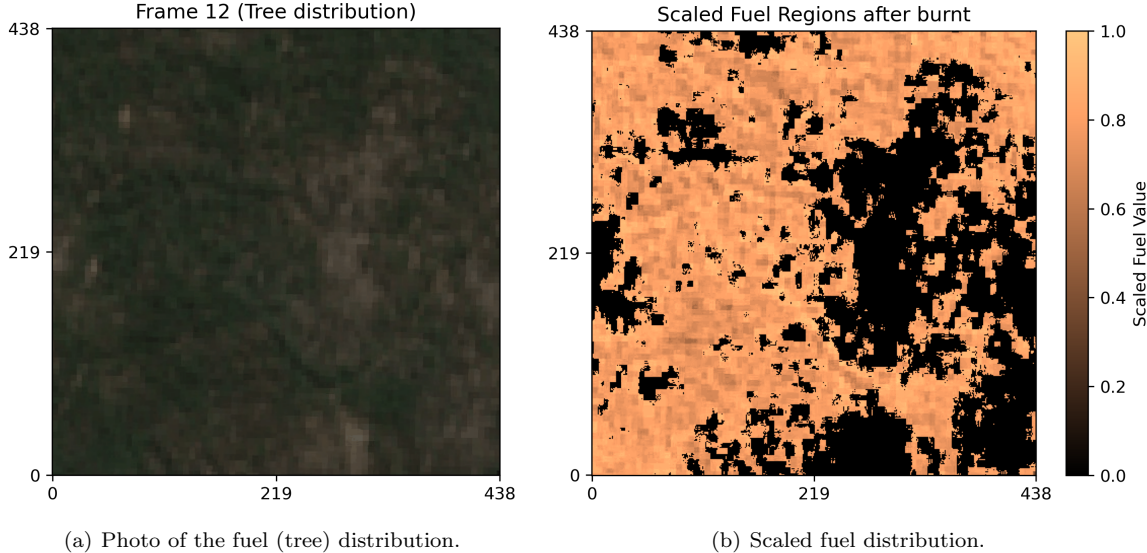
Moreover, our model demonstrates its capability to validate results based on sensitivity to wind speed and combustibility (activation energy), which align with real-life expectations. As wind speed increases, the burning rate goes higher, leading to a faster progression of the fire and a quicker consumption of the forest fuel. Additionally, with higher combustibility (higher activation energy), trees burn more quickly and can sustain for longer durations, resulting in a larger burnt area. We note that in capturing sensitivities especially to wind speeds (which have the same range of values across PDE and ABM models), PDE behavior is more sensitive to changes in wind speed than the ABM as the physics surrounding it is captured into the PDE model.



(a) Burnt area with different wind speeds.

(b) Burnt area with different combustibilities.

Figure 10: ABM Analysis.



(a) Photo of the fuel (tree) distribution.

(b) Scaled fuel distribution.

Figure 11: After-burnt fuel distribution.

Models	Simulated Burnt %	Reference Burnt %
PDE	36.27%	36.68%
ABM	$\approx 80\%$	36.68%

Table 1: Validation Table.

## 7 Conclusion

In this study, we implemented and analyzed two distinct models—PDE-based and ABM-based—for simulating wildfire propagation. The results demonstrate that the PDE model, which captures the underlying

physics of fire spread, provides a more accurate and detailed representation of the burnt area, including the influence of terrain, wind, and fuel dynamics. The ABM, while simpler and more heuristic, yields results with greater radial symmetry and overestimates the burnt area compared to the reference data. We perform a sensitivity analysis of model by capturing burned area with time across wind speeds and combustibility to help validate the simulation models. We note that while our objective is to verify the model by assessing its predictive capabilities on a real world data set comprising of California 2018 wildfires, the sparsity of satellite recordings, uncertainty in vegetation, meteorological conditions, and the ignition point of fire, make the task challenging. Despite discrepancies arising from limitations in data resolution and modeling assumptions, the comparative analysis underscores the strengths and trade-offs of each approach.

## 7.1 What have we learnt?

The first thing we learned was that the choice of hyperparameters is important. For instance, choosing  $dt$  and  $dx$  should ensure compliance with the CFL stability condition. Similarly, other parameters, such as wind speed and topography, derived from real-world data sources, required non-dimensionalization to integrate into our models. What's more, during the data acquisition, we learned how to process the photos by identifying specific pixel characteristics using the RGB filter. like the firing and fuel (tree) positions. Of course, by doing the simulation itself, we got more hands-on experience with coding mathematical models like PDE and ABM models. It gave us a deeper understanding of the forest fire model happening in real life and also inspired us in our own research areas on dealing with different models of one thing.

## 7.2 Future Work

For the data, incorporating higher-resolution satellite imagery, with detailed vegetation maps, and real-time weather data could significantly improve model fidelity. Advances in remote sensing and geospatial analysis could provide more reliable inputs for fire behavior prediction. For the ABM model, we could perform CA in conjunction with online parameter search for robustness. For the PDE model, currently, it is a very simplified model with limited PDEs and parameters. To achieve more accurate results in the future, we suggest including more parameters and looking at the references we provided to include the complete PDEs. Combining the strengths of both PDE-based and ABM-based models could improve overall accuracy and computational efficiency. For instance, the PDE model could be used for large-scale dynamics, while ABMs could refine localized effects, such as fire spread through specific vegetation types.

## References

- [1] National Bureau of Statistics of China, “National data,” 2024, accessed: 2024-11-29.
- [2] A. G. McArthur, “Prescribed burning in australian fire control,” *Australian Forestry*, vol. 30, no. 1, pp. 4–11, 1966.
- [3] Z. Wang, “Measurement method of initial spread rate of hill fire,” *Mountain Research*, vol. 02, p. 4, 1983, [In Chinese].
- [4] A. Chen, F. Ding, G. Zhou, and et al., “A simulation model of forest fire spread based on group intelligence,” *Journal of Systems*, n.d., details such as volume, issue, and pages are missing.
- [5] R. C. Rothermel, *A mathematical model for predicting fire spread in wildland fuels*. Intermountain Forest & Range Experiment Station, Forest Service, US . . . , 1972, vol. 115.
- [6] E. Pastor, L. Zárate, E. Planas, and J. Arnaldos, “Mathematical models and calculation systems for the study of wildland fire behaviour,” *Progress in Energy and Combustion Science*, vol. 29, no. 2, pp. 139–153, 2003.
- [7] B. Drossel and F. Schwabl, “Self-organized criticality in a forest-fire model,” *Physica A: Statistical Mechanics and its Applications*, vol. 191, no. 1-4, pp. 47–50, 1992.
- [8] B. Chopard and M. Droz, “Cellular automata model for the diffusion equation,” *Journal of statistical physics*, vol. 64, pp. 859–892, 1991.
- [9] I. Karafyllidis and A. Thanailakis, “A model for predicting forest fire spreading using cellular automata,” *Ecological Modelling*, vol. 99, no. 1, pp. 87–97, 1997.
- [10] R. M. Almeida and E. E. Macau, “Stochastic cellular automata model for wildland fire spread dynamics,” in *Journal of Physics: Conference Series*, vol. 285, no. 1. IOP Publishing, 2011, p. 012038.
- [11] T. Ghisu, B. Arca, G. Pellizzaro, and P. Duce, “An improved cellular automata for wildfire spread,” *Procedia Computer Science*, vol. 51, pp. 2287–2296, 2015.
- [12] R. Montenegro, A. Plaza, L. Ferragut, and M. Asensio, “Application of a nonlinear evolution model to fire propagation,” *Nonlinear Analysis*, vol. 30, no. 5, pp. 2873–2882, 1997.
- [13] M. Asensio and L. Ferragut, “On a wildland fire model with radiation,” *International Journal for Numerical Methods in Engineering*, vol. 54, no. 1, pp. 137–157, 2002.
- [14] L. Ferragut, M. Asensio, and S. Monedero, “Modelling radiation and moisture content in fire spread,” *Communications in Numerical Methods in Engineering*, vol. 23, no. 9, pp. 819–833, 2007.
- [15] J. Mandel, L. S. Bennethum, J. D. Beezley, J. L. Coen, C. C. Douglas, M. Kim, and A. Vodacek, “A wildland fire model with data assimilation,” *Mathematics and Computers in Simulation*, vol. 79, no. 3, pp. 584–606, 2008.
- [16] S. Eberle, W. Freedon, U. Matthes, F. Willi, M. Nashed, and S. Thomas, “Forest fire spreading,” *Handbook of Geomathematics*, pp. 1349–1385, 2015.
- [17] D. San Martin and C. Torres, “2d simplified wildfire spreading model in python: From numpy to cupy,” *CLEI electronic journal*, vol. 26, no. 1, pp. 5–1, 2023.
- [18] L. Ferragut, M. I. Asensio, and S. Monedero, “A numerical method for solving convection–reaction–diffusion multivalued equations in fire spread modelling,” *Advances in Engineering Software*, vol. 38, no. 6, pp. 366–371, 2007.

- [19] M. Asensio and L. Ferragut, “On a wildland fire model with radiation,” *International Journal for Numerical Methods in Engineering*, vol. 54, no. 1, pp. 137–157, 2002.
- [20] Z. Fangrong, G. Yuning, Q. Guochao, M. Yi, and W. Guofang, “Multi-factor coupled forest fire model based on cellular automata,” *Journal of Safety Science and Resilience*, vol. 5, no. 4, pp. 413–421, 2024.
- [21] X. Rui, S. Hui, X. Yu, G. Zhang, and B. Wu, “Forest fire spread simulation algorithm based on cellular automata,” *Natural hazards*, vol. 91, pp. 309–319, 2018.
- [22] S. Hub, “Sentinel hub: Satellite imagery and services,” 2024, accessed: 2024-12-02. [Online]. Available: <https://www.sentinel-hub.com/>
- [23] European Space Agency, “Copernicus open access hub,” 2024, accessed: 2024-12-02. [Online]. Available: <https://spacedata.copernicus.eu/>
- [24] Meteostat, “Los angeles weather data (july 11, 2018 - august 15, 2018),” 2018, accessed: 2024-12-02. [Online]. Available: <https://meteostat.net/en/place/us/los-angeles?s=KHHR0&t=2018-07-11/2018-08-15>

## A Division of Labor

The division of labors is done equally and shown as follows:

- Data curation: Avasarala, Srikanth (Sentinel-L1A and Digital Elevation Model (DEM) data curation) and Ray, Pranoy (Meteorological data curation, and post-processing data)
- PDE: An, Xiaodong (Model conceptualization and implementation)
- ABM: Ray, Pranoy (Model conceptualization, implementation), Avasarala, Srikanth (Model conceptualization and implementation)
- Git Repository: An, Xiaodong (Setup and Collaborator), Avasarala, Srikanth (Collaborator), Ray, Pranoy (Collaborator)

## B Declaration on the use of AI for writing

The authors declare to have used ChatGPT to clean up the writing for spelling and grammar, but nevertheless have proof-read the manuscript and are responsible for the content of the manuscript.